APPENDIX S1

Fragmentation of Atlantic Forest has not affected gene flow of a widespread seed-dispersing bat

Eve S. McCulloch, J. Sebastián Tello, Andrew Whitehead, Claudia María José Rolón-Mendoza, Mario César D. Maldonado-Rodríguez, and Richard D. Stevens

Contents

Supplementary Methods

Field work

At each of 19 study sites, ten mist nets were set up, open 1900hrs-2400hrs and checked every half hour, for 1-6 consecutive nights. Captured *A. lituratus* were removed from nets and kept in individual cloth bags until they were either released or euthanized (Gannon *et al.* 2007). All handling was conducted according to the Louisiana State University (LSU) animal care and use protocol number 08-040 and followed guidelines of the American Society of Mammalogists (Sikes *et al.* 2011). Voucher specimens will be deposited in the LSU Museum of Natural Sciences and in public collections in the country of origin: Museo Nacional de Historia Natural el Paraguay (MNHNP) in San Lorenzo, Paraguay, and Instituto Miguel Lillo in Tucumán, Argentina.

Polymerase chain reaction (PCR) and genotyping

Fifteen microsatellite loci were genotyped (Table S2): loci AjA40, 80 & 151 were developed by Ortega *et al.* (2002) for *A. jamaicensis*; other markers were developed by McCulloch & Stevens (2011) from *A. lituratus* sequence data. A universal M13 primer tail (Schuelke 2000: TGTAAAACGACGGCCAGT) was added to forward primers, except for loci AjA-151 & AjA-40, which were individually labeled with fluorescent dyes (HEX [reverse primer labeled] and TET, respectively). Schuelke's (2000) suggestion that primers with an M13 tail (forward primer) be used at $1/4^{th}$ volume of the other two primers (reverse primer, and fluorescently labeled universal M13 primer) was followed. For PCR, each locus was amplified in a final volume of 20 uL with the following components: 1 uL of 10-360 ng/uL DNA template, 1 uL of 1.5 U Taq DNA polymerase, 1 uL each of 20 uM reverse primer and universal fluorescently-labeled M13, 0.25 uL forward primer (with M13 tail), 0.96 uL of 25 nM MgCl2, 2 uL of 10x PCR buffer, 0.4 uL of 10 nM dNTP, and autoclaved Nanopure H2O to reach final volume. Thermocycler programs were as follows: Cycling conditions for AjA151 and AjA80 were 5 min at 95°C, followed by 30 cycles of 95°C for 45s, 56°C for 45s, 72°C for 45s, followed by 8 cycles of 95°C for 45s, 53°C for 45s, 72 for 45s, and a final step of 64°C for 45 min. Cycling conditions for AjA40 were 5 min at 95°C, followed by 30 cycles of 95°C for 45s, 50°C for 45s, 72°C for 45s, and a final step of 64°C for 45 min. Cycling program for all other loci (from McCulloch & Stevens [2011]) was 5 min at 94°C, followed by a step-down procedure for 10 cycles of 94°C for 30s, 60°C-50°C (bump down 1°C every cycle) for 45s, 72°C for 1 min, followed by 25 cycles of 94°C for 35s, 50°C for 45s, 72°C for 1 min, and a final step of 72°C for 10 min. PCR product was duplexed for genotyping. Samples were genotyped with a 3130XL Genetic Analyzer (Applied Biosystems) at the LSU Genomics Facility, using ROX 400 Ladder (Applied Biosystems). All alleles were scored by ESM. Sizes were determined in GeneMapper version 4.0 (Applied Biosystems) and scoring was semi-automated: bin sets were established to aid in scoring, but all reads were individually inspected.

Missing data

Missing data for locus AjA80 was replaced with alleles randomly chosen from the global pool of AjA80 alleles, where the probability of being chosen corresponded to the allele's global frequency (across all sites). To assess whether this random-draw replacement was creating

artificial structure due to rare alleles, PCA distances calculated using this modified (random-draw replacement) dataset were correlated with PCA distances calculated using the original (unmodified) dataset, but in which missing allele data for locus AjA80 had been replaced—after transforming the dataset into an allele frequency matrix—with the mean global frequency for that allele (standard missing data option for PCA). The random-draw replacement was done 100 times, and each time the modified dataset was correlated with the original dataset. A Mantel statistic (r_M) > 0.92 (p-value < 0.001) was found each time (example in Figure S2), and there were no indications of artificial structure. Thus, all genetic analyses were conducted using the modified (random-draw replacement for locus AjA80) dataset.

Bayesian analyses

Bayesian analyses can provide an estimate of the "true" number of populations ("clusters": *K*) when there is clear signal in the genetic data. To estimate *K*, we used "Structure" (Pritchard *et al.* 2000) and the R package "Geneland" (Guillot *et al.* 2005). Both methods determine *K* by maximizing HWE and linkage disequilibrium within clusters, but Geneland utilizes individual spatial coordinates in addition to genotypic data. Structure was run under the correlated allele frequency and admixture models (Falush *et al.* 2003), and the following settings: lambda: 0.5, separate alpha per cluster, burn-in: 200000, one million MCMC reps, and used sampling locality information (Hubisz *et al.* 2009). Other parameters were set to default. We tested K = 1 - 14, with five runs at each K. Geneland was run with a correlated allele frequency model and 2 million MCMC iterations, saving every 500 iterations (4000 saved, burn-in: 800). We followed suggestions from the manual and Guillot (2008) for parameterizing function "MCMC." We tested K = 1 - 4, for five runs at each K. Additional runs were planned for *K* with the highest posterior probability; however, only one cluster was inferred (Figure S5).

Effects of underestimating bat density

Underestimating population sizes could increase the perceived effect of drift, which can lead to biased estimates of genetic structure. If bat density were underestimated in the study system, simulations might show greater genetic structure due to drift rather than reduced migration, given a particular level of fragmentation. Thus, additional simulations were run using large densities to determine whether these yielded substantively different results than using small densities. Unfortunately, using bat densities larger than 4 bat/ha for a complete set of simulations (15 populations) required prohibitively great computer power. We therefore simulated an artificial set of 3 sites with large bat densities (20 bats/ha), and compared it to simulations based on the same bat density used in our main set of simulations (4 bats/ha) for those same 3 sites. For these simulations, area and inter-site distances for the 3 simulated sites were calculated as average area and less than the average inter-patch distances of empirical sites (Table S4). These analyses showed that the effect of increasing bat density from 4 bats/ha to 20 bats/ha is minimal and unlikely to change conclusions of our main set of simulations (Figure S4). Therefore, while much larger than predicted population sizes (>20 bats/ha) could contribute to empirical patterns of low differentiation, our data suggests that such effects are not so great as to account for patterns described here.

Tests for statistical power

Low statistical power can be caused by either small sample sizes or very small effect sizes (Sokal & Rohlf 1994). Because our study was limited by sampling effort, it is possible that the lack of a significant difference in genetic structure between fragmented and continuous landscapes could be caused by low sample size, rather than by the true absence of a fragmentation effect. To confirm our results were not spurious, we tested the power of our analyses in multiple ways. First, we used simulations described in the main body of the manuscript to demonstrate that—using the same sample size used in our dataset—fragmentation should lead to high levels of genetic structure, in the form of high F_{ST} values and strong IBD trends. As described in the main manuscript, simulated fragmentation is inconsistent with our empirical data. To further demonstrate that our conclusions are appropriate, we designed a power test for the PERMDISP procedure, which compares the magnitude of F_{ST} values between sites in the fragmented and continuous landscapes:

To evaluate the power of the PERMDISP test given our sample sizes, we constructed power curves (Sokal & Rohlf 1994), following the subsequent steps:

1) A new set of artificial fragmented distances was produced by:
    a. Sampling with replacement from the empirical distances among continuous sites. The number of sampled distances was equal to the number of empirical distances among sites in the fragmented landscape (i.e., 14 in the "*all frag*." set, and 5 in the "*best frag."* set).
    b. Multiplying the randomly sampled distances by a factor, *M*. When the value of *M* is less than 1, the artificial fragmented distances are smaller than distances among continuous sites. When *M* is equal to 1, both artificial fragmented and empirical continuous distances come from the same distribution of bootstrapped distances. When *M* is greater than 1, artificial fragmented distances are larger than the distances among continuous sites.
2) The PERMDISP test was conducted using empirical continuous and artificial fragmented distances, and the p-value of this test was saved.
3) Steps above were repeated 500 times creating a distribution of p-values expected given the difference between artificial fragmented and empirical continuous distances produced by the multiplier *M*.
4) We estimated statistical power as the proportion of times the PERMDISP analysis was statistically significant given *M* using an alpha of 0.05.
5) We repeated the steps above for 50 values of M, evenly spaced between 0.1 and 15, including 1.
6) The power curve was then produced by plotting statistical power for each value of *M* against the expected effect size, calculated as the difference between the mean expected fragmented distances given *M*, minus the mean empirical continuous distances.

Finally, we added to the power profile the empirical effect size (i.e., mean distance of empirical fragmented sites minus mean distance of empirical continuous sites), and the effect sizes produced by the simulation models given various levels of reduction in migration rates (i.e., mean distance of simulated fragmented sites minus mean distances of empirical continuous sites). These analyses were produced for geographic distances and for F_{ST} values, and for the analyses using the "*all frag.*" and "*best frag*." site sets in the fragmented landscape.

Figure S3 shows the results. As expected, the power of the test increased with an increase in effect size, and the increase was faster for analyses that included a larger sample size (i.e.,

when using the "*all frag*." set of fragmented sites: Figure S3A-C). For geographic distances, the power of the PERMDISP test is only moderate when using the "*best frag*." set (Figure S3D), but is very good when using all fragmented sites (Figure S3A). This change in power is mostly due to an increase in the empirical effect size. For F_{ST} values in the empirical data, the power of the test is very low irrespective of the set of fragmented sites being used. However, the power profile and the simulated effect sizes confirm that, when using all fragmented sites, this lack of power is due to a very low effect size, rather than to low sample size. In all cases, the empirical effect size is extremely close to zero, and consequently the power of the test is close to zero as well. The effect sizes produced by the simulations, however, lead to PERMDISP tests that have a moderate to excellent chance of detecting a significant difference between fragmented and continuous sites (Figure S3B and C). This is true, even if migration rates are very high (m = 0.9 or 0.7). This is also true for analyses of the "best frag." site-set when assuming short distance migrations (Figure S3E). When assuming long distance migrations, however, analyses based on the "*best frag*." set of sites have low statistical power for the empirical data and for most simulated migration rates (Figure S3F). In conclusion, the PERMDISP analyses using the "*best frag*." site-set might not easily distinguish lack of power due to low sample size from a true lack of fragmentation effects. On the other hand, PERMDISP analyses using all sites in the fragmented landscape should be powerful enough to detect even slight effects of fragmentation.

The power analyses we have presented here help support our conclusions. The fact that the PERMDISP analysis using all fragmented sites did not find statistically significant differences between fragmented and continuous landscapes for empirical F_{ST} values, but it did for geographic distances, suggests that there are high rates of migration between patches in the fragmented landscape, likely preventing population differentiation.

Supplementary Tables

Table S1. Site information, abbreviations with no. bats genotyped (N), temperature (Tmin and Tmax) and precipitation data (obtained from WorldClim: www.worldclim.org), as well as heterozygosity (H_S) calculated in "adegenet" (function "Hs"), and no. private alleles (unique to a site). Variation in minimum and maximum temperature (StDev) was similar for all sites (3.6°C and 3.4°C, respectively). Sites situated in continuous forest in Misiones, Argentina are Igz1, Igz2, Igz3, Urug, and Yate. Five sites situated in the fragmented landscape of eastern Paraguay and used for direct comparison to continuous sites are Itab, Limo, Maha, Piky, and Tati. PP: Parque Provincial (State Park), PN: Parque Nacional (National Park), RB: Refugio Biológico (Biological Refuge), R: Reserva (Reserve), E: Estancia (Ranch), RN: Reserva Natural (Nature Reserve), PY: Paraguay, AR: Argentina

Site	Abbrev. (N)	Country (State)	Management	Long.	Lat.	Elev (m)	Tmin (°C)	Tmax (°C)	Prec. (mm)	Var. Prec. (mm)	Date	Hs	No. Alleles	Priv. Alleles
E. Arakangy	Arak (28)	PY (Caaguazú)	Private landowner	-55.59808	-24.53959	255	16.30	27.59	127.23	31.98	Mar-09	0.77	142	3
RB Carapa	Cara (27)	PY (Canindeyú)	Itaipu Binacional	-54.37694	-24.37177	256	15.19	27.49	134.99	30.66	Jan-09	0.75	134	1
RN Privada Cerrados de Tagatiya (E. Garay Cue)	Cerr (24)	PY (Concepción)	Massimo & Angela Coda	-57.28460	-22.74496	189	17.87	29.46	114.48	46.88	Feb-08 (7), Mar-09 (17)	0.79	138	1
R. Guyra Reta (PN San Rafael)	Guyr (34)	PY (Itapúa)	Guyra Paraguay	-55.78692	-26.52018	169	15.09	27.62	137.17	31.64	Feb-09	0.78	149	3
PN Iguazú	Igz1(19)	AR (Misiones)	National Parks Service	-54.47850	-25.68220	235	14.23	27.56	144.08	25.94	Apr-09	0.77	136	0
PN Iguazú	Igz2 (27)	AR (Misiones)	National Parks Service	-54.44741	-25.74535	242	14.07	27.49	144.42	26.31	Apr-09	0.78	143	4
PN Iguazú	Igz3 (26)	AR (Misiones)	National Parks Service	-54.40028	-25.64692	208	14.37	27.65	144.34	33.07	Apr-09	0.76	135	2
RB Itabo	Itab (19)	PY (Alto Paraná)	Itaipu Binacional	-54.70311	-25.05982	270	14.94	27.02	136.87	29.15	Jan-08	0.77	126	1
RN Kaí Ragüe	KaiR (19)	PY (Amambay)	Massimo & Angela Coda	-56.25228	-23.28971	193	17.22	28.80	120.23	41.85	Feb-08	0.77	124	0
RB Limoy	Limo (32)	PY (Alto Paraná)	Itaipu Binacional	-54.45315	-24.75069	250	14.52	27.26	135.68	29.11	Jan-08	0.77	145	1
RN Maharishi	Maha (29)	PY (Alto Paraná)	Maharishi Country of World Peace S.A.	-54.63080	-25.56290	206	15.06	27.68	142.17	23.51	Mar-09	0.78	146	0
RN del Bosque Mbaracayú (RNBM: Central Station)	Mba1 (26)	PY (Canindeyú)	Fundación Moisés Bertoni	-55.50383	-24.12587	186	16.78	28.16	134.94	36.51	Feb-09	0.79	143	3
RN Privada Morombí (E. Golondrina)	Moro (27)	PY (Caaguazú)	Campos Morombí S.A.C.A. (Grupo Riquelme)	-55.39598	-24.66280	283	16.03	27.48	130.68	33.20	Feb-08 (13), Mar-09 (14)	0.79	146	3
RB Pikyry	Piky (34)	PY (Alto Paraná)	Itaipu Binacional	-54.51331	-25.19949	233	14.89	27.15	140.11	30.28	Jan-09	0.77	151	0
RB Mbaracayú (Salto)	Salt (41)	PY (Canindeyú)	Itaipu Binacional	-54.30590	-24.04641	259	16.04	27.59	133.95	38.14	Jan-09	0.79	173	2
RN Privada Tapyta	Tapy (30)	PY (Caazapá)	Guyra Paraguay	-55.80205	-26.27137	202	15.00	27.27	133.36	33.58	Feb-09	0.80	151	0
RB Tati Yupi	Tati (25)	PY (Alto Paraná)	Itaipu Binacional	-54.58327	-25.36409	223	15.32	27.44	141.41	28.30	Jan-09	0.77	138	0
PP Urugua-í	Urug (31)	AR (Misiones)	State Park Services	-54.17043	-25.85995	303	13.18	26.72	146.00	30.54	May-09	0.78	136	1
RN Privada Yate-í	Yate (28)	AR (Misiones)	Conservacion Argentina	-53.98210	-25.85749	383	12.57	26.01	149.25	31.75	May-09	0.78	136	1

Table S2. Descriptions of loci including name used in text, repeat motif (Rep.), original ID (only applicable for primers from McCulloch & Stevens [2011]), primer sequence, no. alleles (A), size range (bp) for *A. lituratus*, expected and observed heterozygosity across sites (calculated in adegenet for 14 loci included in analyses), and F_{IS} calculated in Genepop v4.0.10. Loci AjA40, 80 & 151 were developed by Ortega *et al.* (2002) for *A. jamaicensis*; other markers were developed by McCulloch & Stevens (2011) from *A. lituratus* sequence data. Locus N29507 was excluded from genetic structure analyses due to high F_{IS}, and was out of HWE.

Name	Rep.	ID		Sequence	A	Size Range (bp)	HE	HO	F_{IS}
AjA151	GT	NA	F:	GGGTGGAAAGGGAGAGAAAA	27	134-186	0.91	0.90	0.02
		NA	R:	AAGCTCTTCCCTGACCACTTA					
AjA40	GT	NA	F:	GATGTGAATGGTGTTTTTAGAGCTT	19	184-226	0.75	0.74	0.05
		NA	R:	CTCTACAGTGGACCCACATCATT					
AjA80	CA	NA	F:	ATGTGCTCAATCCACTGAACTAGA	20	125-165	0.90	0.88	0.03
		NA	R:	ATCCACTGACAGATGAATGGATAAA					
F05378	TCTG	AL2_05378	F:	CCAGGTCAGCCAAGGTAACG	18	151-201	0.90	0.83	0.08
		AL2_13822	R:	TGGGAGAAAGAGAGTTGGGC					
F13578	AAC	AL2_13578	F:	AGGCGGTCATGTAAGTTGGC	14	391-433	0.79	0.80	0.02
		AL2_22124	R:	CTCTACCTGCATGTGGGTGC					
F20293	TGCC	AL2_20293	F:	CCAGTCAAGGTGTGAGCAGG	10	402-438	0.68	0.71	-0.02
		AL2_18937	R:	TGGGATATGGGAAGTGAGGG					
F25023	AATC	AL2_25023	F:	GTTGCAGGTTCAATCCTCCC	14	142-210	0.66	0.66	0.03
		AL2_06886	R:	CTCAACCCACTGAGCACACC					
F27850	AATG	AL2_27850	F:	TCCACAGCTAAGGGACTAACCC	13	220-272	0.78	0.78	0.01
		AL2_25954	R:	TGGCCTTTCAATTACACCCC					
N00821	ATGG	AL2_00821	F:	CAGAGGCAGGTCAAAGGAGG	13	263-319	0.87	0.83	0.08
		AL2_06824	R:	GCCATATGCTTCTTGCTCCC					
N01230	TC	AL2_01230	F:	AATGCAAATCAAATGCAGCC	24	223-287	0.86	0.80	0.09
		AL2_24257	R:	TTTGTTCTCCAGCCTTGTTCC					
N05700	AACT	AL2_05700	F:	CTTTCCTTCCACACCCAACC	15	273-367	0.75	0.77	0.01
		AL2_16761	R:	GTGCCTCTGAGGAGGATGC					
N11949	ATT	AL2_11949	F:	GAGGCCACAGAAGCTGAAGG	20	354-416	0.78	0.75	0.06
		AL2_13284	R:	GGTCCACAATGGAGGATAAGG					
N16384	ATCT	AL2_16384	F:	GGGCCAAATCCAATGAGTAGC	28	190-312	0.91	0.88	0.05
		AL2_12662	R:	CCTGCCACTTGGTAGGTTGG					
N25522	AAAT	AL2_25522	F:	GCTAGGTATGGGGCTGTATTCC	15	234-288	0.60	0.63	-0.01
		AL2_16051	R:	CACCTTCTGGCCTCAATTCC					
N29507	AAAC	AL2_29507	F:	GCTGGGACAGTTCAGGTTCC	14	283-325			0.16
		AL2_02049	R:	TTTGGACAGCAAACCACTCG					

Table S3. Pairwise geographic distances between sites in meters. Sites situated in continuous forest (Misiones, Argentina) are Igz1, Igz2, Igz3, Urug, and Yate. Five fragmented landscape (Paraguay) sites used for comparison to continuous sites are Itab, Limo, Maha, Piky, and Tati.

	Arak	**Cara**	**Cerr**	**Guyr**	**Igz1**	**Igz2**	**Igz3**	**Itab**	**KaiR**	**Limo**	**Maha**	**Mba1**	**Moro**	**Piky**	**Salt**	**Tapy**	**Tati**	**Urug**	**Yate**
Arak		125200	262892	220232	169620	176922	172177	107283	153623	118246	149587	46813	24601	131759	142100	192939	137275	205171	218719
Cara			347241	277043	145522	152322	141272	83053	225538	42676	134411	117638	108185	92717	36752	254691	111880	166163	169328
Cerr				444802	432510	439810	434917	367175	121810	364223	412472	237702	286721	391707	336864	418494	399521	467905	480828
Guyr					160465	159101	169130	194908	360919	237415	156957	266764	209478	194175	311994	27609	175897	177361	194770
Igz1						7660	8772	72557	320231	103221	20215	201122	145965	53589	182035	147736	36781	36644	53448
Igz2							11886	80181	327765	110186	27342	208724	153361	60832	188735	147603	44388	30541	48290
Igz3								71827	321582	99424	24957	202042	148196	50854	177546	156508	36334	32996	48004
Itab									251427	42548	56203	131448	82688	24612	119247	173744	35804	103570	114309
KaiR										244301	300719	120007	175278	275554	215511	333400	285447	354274	365736
Limo											91738	127048	95899	50084	79425	216253	69206	126136	131464
Maha												182002	126085	41959	171163	141173	22537	56725	72827
Mba1													60471	155548	122127	239562	165780	234557	245749
Moro														107158	129984	182815	112979	181184	194421
Piky															129438	175562	19548	80877	90357
Salt																288956	148631	201355	203264
Tapy																	158231	169504	187792
Tati																		68827	81449
Urug																			18880
Yate																			

Table S4. Spatial coordinates and predicted population sizes for Easypop simulations: coordinates (based on empirical data), approximate area (for 2010 as reported by reserve management, and predicted area for 1960), proportion of remaining Paraguayan APAF represented by each site (present), and population sizes used to parameterize Easypop simulations for (A) 15 populations based on empirical sites and (B) 3 artificial populations. Effective population sizes (Ne) were calculated based on population density of (A/B) 4 or (B) 20 bats/ha, and Storz *et al.*'s (2001) N_e/N ratio (see main manuscript Methods for details).

				2010		1960		
	Site	**Latitude**	**Longitude**	**Approx. Area (ha)**	**% Forest**	**Area (ha)**	**Predicted N_e (4 bats/ha)**	**Predicted N_e (20 bats/ha)**
	Igz/ Igz2/ Igz3/ Urug/Yate	-25.758377	-54.295752	1000000	NA	1000000	1680000	
	Arak	-24.539579	-55.598080	1000	0.06%	4371	7400	
	Cara	-24.371775	-54.376958	3250	0.19%	14204	23800	
	Cerr	-22.744962	-57.284580	5000	0.29%	21853	36800	
	Guyr	-26.520224	-55.786888	64000	3.76%	279718	470000	
	Itab	-25.059809	-54.703089	15200	0.89%	66433	111600	
	KaiR	-23.289731	-56.252293	9000	0.53%	39335	66000	
A)	Limo	-24.750688	-54.453137	14800	0.87%	64685	108600	
	Maha	-25.562910	-54.630750	300	0.02%	1311	2200	
	Mba1	-24.061181	-55.425154	67000	3.94%	292829	492000	
	Moro	-24.662789	-55.395982	25000	1.47%	109265	183600	
	Pikyr	-25.199462	-54.513287	800	0.05%	3496	5800	
	Salt	-24.046389	-54.305867	1356	0.08%	5927	10000	
	Tapy	-26.271387	-55.802081	4700	0.28%	20542	34600	
	Tati	-25.364108	-54.583260	2245	0.13%	9812	16400	
	Artificial Pop1	-25.178833	-56.139459	NA	NA	128919	108300	541450
B)	Artificial Pop2	-25.198945	-54.504804	NA	NA	128919	108300	541450
	Artificial Pop3	-25.188889	-55.322132	NA	NA	128919	108300	541450

Table S5. Pairwise measures of genetic differentiation: Nei 1973's F_{ST} (upper half) and Jost's D (lower half). F_{ST} values were calculated in the R package "adegenet" (Jombart 2008) and Jost's D in "DEMEtics" (Gerlach *et al.* 2010). Jost's D values in dark grey fill & bold text are significant (p-value < 0.05) and light-gray fill & italicized text indicate marginally significant (0.05 < p-value < 0.1).

	Arak	**Cara**	**Cerr**	**Guyr**	**Igz1**	**Igz2**	**Igz3**	**Itab**	**KaiR**	**Limo**	**Maha**	**Mba1**	**Moro**	**Piky**	**Salt**	**Tapy**	**Tati**	**Urug**	**Yate**
Arak		0.012	0.012	0.008	0.012	0.011	0.011	0.014	0.013	0.015	0.010	0.010	0.013	0.007	0.009	0.012	0.015	0.012	0.013
Cara	*0.068*		0.013	0.008	0.014	0.014	0.013	0.014	0.014	0.011	0.014	0.013	0.012	0.010	0.007	0.015	0.014	0.015	0.014
Cerr	0.049	0.013		0.009	0.015	0.011	0.015	0.010	0.014	0.015	0.011	0.010	0.011	0.011	0.009	0.010	0.012	0.010	0.011
Guyr	0.055	0.000	-0.008		0.010	0.010	0.010	0.010	0.011	0.010	0.010	0.007	0.008	0.007	0.006	0.011	0.010	0.009	0.008
Igz1	0.077	**0.014**	-0.004	0.008		0.016	0.017	0.017	0.022	0.018	0.019	0.016	0.013	0.010	0.011	0.020	0.018	0.015	0.016
Igz2	0.041	0.025	-0.014	-0.001	0.006		0.011	0.014	0.017	0.012	0.010	0.011	0.011	0.010	0.008	0.013	0.015	0.008	0.009
Igz3	0.058	0.017	0.019	0.009	**0.034**	-0.005		0.014	0.017	0.014	0.014	0.011	0.014	0.010	0.010	0.018	0.014	0.011	0.011
Itab	0.083	0.003	-0.040	-0.018	0.003	-0.013	-0.003		0.016	0.013	0.015	0.012	0.010	0.008	0.010	0.015	0.015	0.008	0.011
KaiR	0.059	-0.011	-0.018	-0.008	0.005	0.005	*0.026*	-0.018		0.013	0.014	0.013	0.014	0.012	0.011	0.012	0.017	0.014	0.015
Limo	**0.115**	*0.017*	**0.043**	0.011	**0.055**	*0.021*	**0.041**	0.018	0.003		0.014	0.012	0.012	0.011	0.010	0.016	0.013	0.011	0.013
Maha	0.025	**0.032**	0.004	0.016	**0.050**	0.000	*0.029*	0.027	0.005	**0.030**		0.010	0.014	0.012	0.009	0.012	0.015	0.012	0.013
Mba1	0.056	0.016	-0.021	-0.018	*0.034*	0.002	0.010	-0.009	-0.013	0.014	0.013		0.011	0.009	0.007	0.010	0.014	0.008	0.009
Moro	*0.076*	0.006	0.002	-0.013	0.006	0.002	**0.036**	-0.019	0.005	**0.029**	**0.036**	0.008		0.009	0.010	0.014	0.013	0.010	0.010
Piky	0.062	0.005	0.012	-0.003	-0.001	0.005	0.007	-0.042	0.001	**0.030**	*0.022*	0.013	0.007		0.007	0.011	0.013	0.007	0.010
Salt	0.047	-0.001	0.001	-0.009	0.011	-0.006	0.017	-0.013	-0.006	**0.029**	0.007	-0.001	0.013	-0.001		0.008	0.010	0.008	0.009
Tapy	*0.082*	**0.044**	0.003	*0.024*	**0.059**	0.013	**0.063**	0.026	-0.014	**0.039**	0.017	0.014	**0.047**	**0.028**	-0.005		0.013	0.010	0.013
Tati	**0.110**	**0.027**	0.013	0.014	*0.034*	**0.030**	**0.039**	0.017	0.020	*0.023*	**0.055**	**0.045**	0.024	**0.044**	**0.030**	*0.029*		0.014	0.012
Urug	**0.077**	**0.029**	-0.002	-0.004	*0.025*	-0.014	0.008	-0.027	0.008	*0.022*	*0.023*	0.001	0.007	-0.003	0.006	0.012	**0.035**		0.009
Yate	**0.087**	**0.036**	-0.002	-0.003	*0.032*	-0.012	0.008	-0.034	0.011	*0.022*	*0.029*	-0.006	-0.003	0.011	0.018	**0.035**	0.015	-0.003	

Table S6. Pairwise genetic distances between sites: CSE (upper half) and PCA (lower half). CSE distances were calculated in Genetix, all are significant (p-value < 0.05). PCA distances calculated in R package "adegenet" (Jombart 2008) for individuals. Axes explaining 80% of variation in the dataset were kept and used to calculate new PC coordinates for sites by averaging individual coordinates for each site.

	Arak	**Cara**	**Cerr**	**Guyr**	**Igz1**	**Igz2**	**Igz3**	**Itab**	**KaiR**	**Limo**	**Maha**	**Mba1**	**Moro**	**Piky**	**Salt**	**Tapy**	**Tati**	**Urug**	**Yate**
Arak		0.021	0.021	0.019	0.027	0.021	0.020	0.026	0.025	0.025	0.019	0.020	0.023	0.018	0.020	0.022	0.024	0.019	0.024
Cara	2.68		0.020	0.017	0.027	0.023	0.019	0.022	0.020	0.019	0.022	0.019	0.019	0.018	0.016	0.021	0.024	0.018	0.022
Cerr	2.77	2.64		0.020	0.023	0.023	0.023	0.019	0.022	0.025	0.023	0.024	0.021	0.022	0.019	0.023	0.024	0.019	0.023
Guyr	2.67	2.25	2.66		0.024	0.020	0.019	0.023	0.020	0.019	0.018	0.018	0.016	0.015	0.015	0.020	0.021	0.016	0.020
Igz1	3.08	2.78	2.86	2.71		0.031	0.030	0.031	0.032	0.032	0.031	0.032	0.027	0.025	0.025	0.030	0.030	0.027	0.028
Igz2	2.95	2.92	2.99	2.82	3.31		0.022	0.027	0.025	0.022	0.020	0.023	0.020	0.019	0.019	0.020	0.023	0.017	0.022
Igz3	2.87	2.66	3.06	2.66	3.02	2.94		0.024	0.024	0.024	0.023	0.023	0.022	0.020	0.019	0.025	0.025	0.018	0.022
Itab	2.93	2.70	2.51	2.60	2.97	3.08	2.95		0.027	0.027	0.027	0.028	0.023	0.020	0.022	0.026	0.028	0.021	0.022
KaiR	2.68	2.37	2.65	2.40	3.04	2.96	2.78	2.86		0.025	0.025	0.026	0.023	0.022	0.022	0.023	0.027	0.022	0.026
Limo	2.82	2.34	2.90	2.26	3.11	2.73	2.79	2.79	2.61		0.022	0.025	0.021	0.020	0.021	0.024	0.021	0.019	0.023
Maha	2.65	2.76	2.77	2.43	3.11	2.74	2.85	2.91	2.69	2.57		0.020	0.022	0.016	0.017	0.020	0.020	0.018	0.022
Mba1	2.92	2.66	2.98	2.49	3.21	3.00	2.89	2.99	2.76	2.74	2.54		0.024	0.020	0.018	0.023	0.028	0.019	0.023
Moro	3.08	2.66	2.86	2.49	2.99	2.86	3.03	2.78	2.66	2.61	2.94	2.91		0.017	0.017	0.021	0.023	0.018	0.021
Piky	2.48	2.36	2.68	2.17	2.74	2.65	2.61	2.52	2.45	2.37	2.39	2.54	2.39		0.016	0.019	0.021	0.013	0.018
Salt	2.63	2.28	2.57	2.15	2.65	2.69	2.69	2.65	2.45	2.50	2.50	2.55	2.56	2.21		0.015	0.019	0.017	0.018
Tapy	2.85	2.75	2.84	2.53	3.09	2.84	3.13	2.95	2.64	2.77	2.62	2.80	2.85	2.53	2.19		0.022	0.018	0.024
Tati	3.21	2.94	3.02	2.86	3.17	3.14	3.20	3.20	3.02	2.67	2.89	3.31	3.12	2.88	2.78	2.96		0.021	0.023
Urug	2.65	2.41	2.61	2.15	2.86	2.54	2.58	2.47	2.51	2.31	2.47	2.45	2.57	1.94	2.25	2.48	2.86		0.018
Yate	2.97	2.80	2.89	2.53	2.88	2.86	2.79	2.82	2.86	2.68	2.74	2.77	2.74	2.39	2.59	2.83	3.00	2.43	

Supplementary Figures

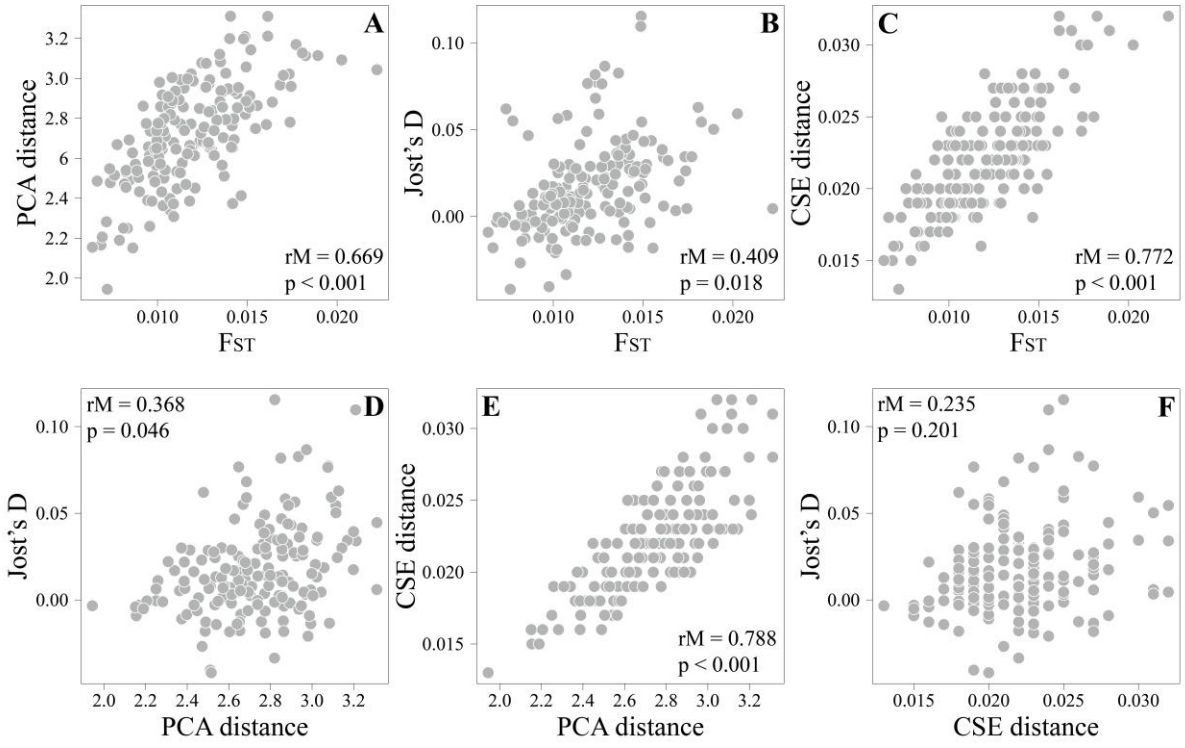

Figure S1. Correlations between 4 metrics of genetic structure measured for all sites at 14 loci. Significance for Mantel tests calculated with 10000 permutations in the R package "ecodist" (Goslee & Urban 2007). Correlation between F_{ST} and all other distances (panels A-C), between CSE and PCA distances (panel E), and between PCA distances and Jost's D (panel D) are statistically significant based on Mantel analyses. Correlation between CSE and Jost's D is positive but not significant (panel F).

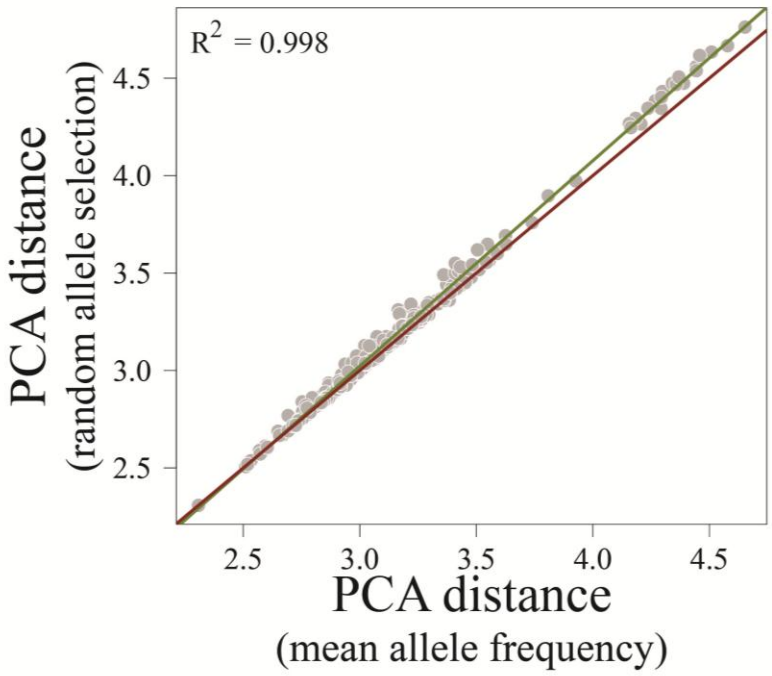

Figure S2. Mantel correlation of PCA results obtained by correlating a modified dataset where missing data for locus AjA80 were replaced by random-draw alleles (where the probability of an allele being chosen corresponded to its global frequency) with PCA results from the unmodified dataset where missing data were replaced with the mean global frequency for the missing allele (default option). The red line is the 1:1 correspondence line and the green is the linear regression line.

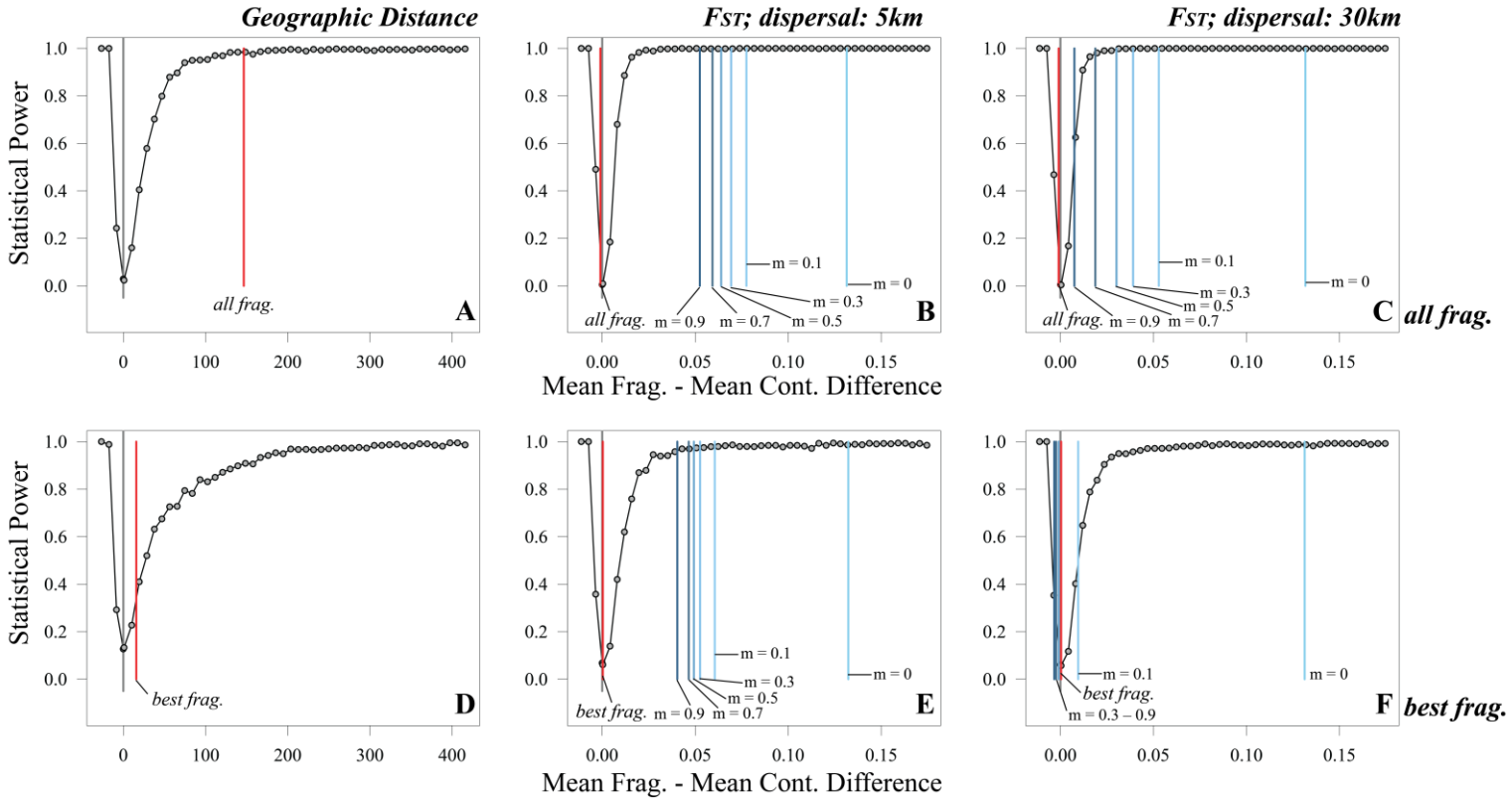

Figure S3. Tests of statistical power for the PERMDISP procedure, using simulated and empirical distances. Panels A-C show results from comparing differences between "*all frag.*" and continuous sites ("*all cont.*"), while panels D-F show results from "*best frag.*" and "*all cont.*" comparisons. Colored horizontal lines show mean differences between F_{ST} values from fragmented (empirical [red] or simulated data [shades of blue representing different simulated levels of migration]), and continuous sites (empirical data). Hollow circles and connecting lines show statistical power. There is little power for detecting a difference between empirical fragmented and continuous sites, regardless of how many fragmented sites are used in the analysis ("*all frag.*" [14 sites] or "*best frag.*" [5 sites]). However, there is very good statistical power for detecting a difference between simulated fragmented and empirical continuous sites using the full set of fragmented sites, even under simulated conditions of high migration and dispersal. Results of these tests indicate that lack of power in our analyses stems primarily from a very small empirical effect size, rather than insufficient sampling.

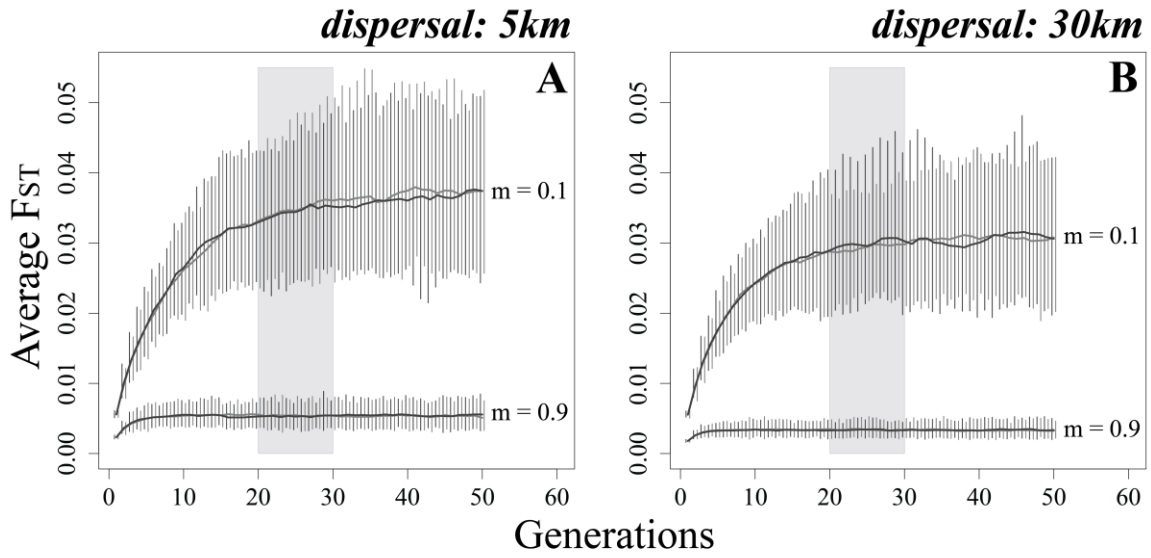

Figure S4. F_{ST} values from Easypop simulations that varied population sizes for 3 artificial sites (128919 ha each) based on population densities of 4 bats/ha (grey lines) and 20 bats/ha (black lines). Two dispersal distances (5km: panel A; 30km: panel B) and migration rates (0.1, 0.9) were simulated. Other parameters are described in the main Methods section of the paper and in Table S4. Vertical lines indicate range of F_{ST} values over 100 replicate simulations for a given generation. The grey bar highlights time span under consideration. Populations with 5 times as many individuals did not differentiate faster than their smaller counterparts, suggesting that what differentiations occur in our main simulation set are not primarily driven by magnitude of genetic drift, barring population sizes considerably larger than those we were able to test.

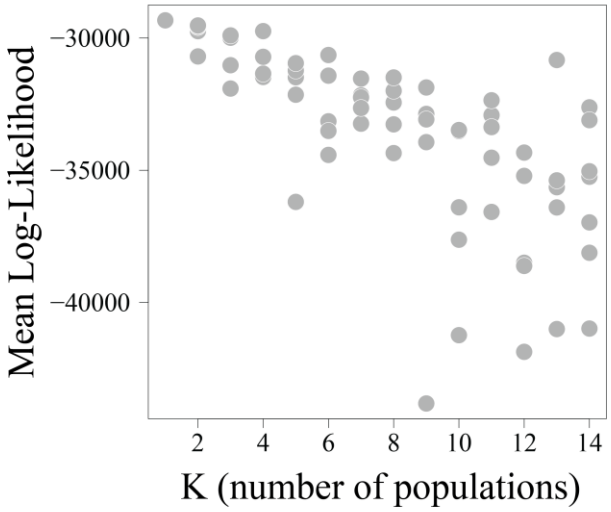

Figure S5. Structure clustering analysis results for K =1 – 14, based on five runs (grey circles) per K. Structure was run under the correlated allele frequency and admixture models (Falush *et al.* 2003), and the following settings: lambda: 0.5, separate alpha per cluster, burn-in: 200000, one million MCMC reps, and used sampling locality information (Hubisz *et al.* 2009).

Supplementary References

Belkhir K, Borsa P, Chikhi L, Raufaste N, Bonhomme F (1996-2004) GENETIX, p. logiciel sous Windows TM pour la génétique des populations. Laboratoire Génome, Populations, Interactions, CNRS UMR 5171, Université de Montpellier II, Montpellier, France.

Cartes JL (2003) Chapter 24: Brief history of conservation in the Interior Atlantic Forest. In: *The Atlantic Forest of South America: Biodiversity status, threats, and outlook* (eds. Galindo-Leal C, Gusmao Camara Id). Island Press, Washington D.C.

Falush D, Stephens M, Pritchard JK (2003) Inference of population structure using multilocus genotype data: Linked loci and correlated allele frequencies. *Genetics* **164**, 1567-1587.

Gannon WL, Sikes RS, Animal Care and Use Committee A (2007) Guidelines of the American Society of Mammalogists for the use of wild mammals in research. *Journal of Mammalogy* **88**, 809-823.

Gerlach G, Jueterbock A, Kraemer P, Deppermann J, Harmand P (2010) Calculations of population differentiation based on GST and D: forget GST but not all of statistics! *Molecular Ecology* **19**, 3845-3852.

Goslee SC, Urban DL (2007) The ecodist package for dissimilarity-based analysis of ecological data. *Journal of Statistical Software* **22**, 1-19.

Guillot G, Estoup A, Mortier F, Cosson JF (2005) A spatial statistical model for landscape genetics. *Genetics* **170**, 1261-1280.

Hubisz MJ, Falush D, Stephens M, Pritchard JK (2009) Inferring weak population structure with the assistance of sample group information. *Molecular Ecology Resources* **9**, 1322-1332.

Jombart T (2008) adegenet: a R package for the multivariate analysis of genetic markers. *Bioinformatics* **24**, 1403-1405.

McCulloch ES, Stevens RD (2011) Rapid development and screening of microsatellite loci for *Artibeus lituratus* and their utility for six related species within Phyllostomidae. *Molecular Ecology Resources* **11**, 903-913.

Ortega J, Maldonado JE, Arita HT, Wilkinson GS, Fleischer RC (2002) Characterization of microsatellite loci in the Jamaican fruit-eating bat *Artibeus jamaicensis* and cross-species amplification. *Molecular Ecology Notes* **2**, 462-464.

Pritchard JK, Stephens M, Donnelly P (2000) Inference of population structure using multilocus genotype data. *Genetics* **155**, 945-959.

Schuelke M (2000) An economic method for the fluorescent labeling of PCR fragments. *Nature: Biotechnology* **18**, 233-234.

Sikes RS, Gannon WL, Animal Care and Use Committee A (2011) Guidelines of the American Society of Mammalogists for the use of wild mammals in research. *Journal of Mammalogy* **92**, 235-253.

Sokal RR, Rohlf FJ (1994) *Biometry: The Principles and Practices of Statistics in Biological Research*, 3rd edn.

Storz JF, Bhat HR, Kunz TH (2001) Genetic consequences of polygyny and social structure in an Indian Fruit Bat, *Cynopterus sphinx*. I. Inbreeding, outbreeding, and population subdivision. *Evolution* **55**, 1215-1223.